Atomization and Sprays, vol. 17, pp. 347–380, 2007

CHARACTERIZATION OF SPLASH-PLATE ATOMIZERS USING NUMERICAL SIMULATIONS

Mohammad P. Fard*
Simulent Inc., Toronto, Canada and Ferdowsi University, Mashhad, Iran

Denise Levesque and Stuart Morrison
ALSTOM Canada Inc., Ottawa, Canada

Nasser Ashgriz and Javad Mostaghimi
University of Toronto, Toronto, Canada

Original Manuscript Submitted: 10/13/04; Final Draft Received: 9/1/2005

A computational model has been developed that can be used for the spray characterization of splash-plate atomizers. The computer model, called BLSpray, can accurately simulate the impingement of a liquid jet on the surface of a splash-plate nozzle, as well as the formation of the liquid film and subsequent droplets. To validate the model, simulation results were compared to experimental measurements for the film thickness and velocity distributions in a typical splash-plate nozzle. Close agreement between numerical results and measurements validated the model and its underlying assumptions. Correlations were developed between liquid film characteristics at the nozzle exit and the spray mean drop sizes. This was done by running many different numerical simulations on a typical splash-plate nozzle using the developed computer code. The correlations were obtained by performing a close inspection of the numerical results in order to extract all information regarding the liquid film and spray. The results of the developed code were combined with the correlations to get the spray drop size distribution in a more practical approach, with less computational time and effort. This capability, along with the program module developed for analyzing the output data, has turned the developed code into an efficient and practical tool in the design and characterization of splash-plate nozzles. The developed computer model can be used to predict the behavior of a flow into a nozzle at different operating conditions, and also as a tool in the design of new nozzles. This paper presents mathematical formulations, results of model validation, and the spray drop size distribution for a typical ALSTOM splash-plate nozzle. Also, the effect of some of the main parameters on the spray pattern, such as nozzle diameter, nozzle angle, and nozzle velocity, are investigated.

*Corresponding author; e-mail: mp2fard@yahoo.ca and siminfo@simulent.com

INTRODUCTION

In a splash-plate atomizer, a flat plate of usually rounded cross section is attached at an angle to the end of a liquid-carrying pipe. When the liquid flowing through the pipe exits from the end, it strikes the flat face of the plate at an angle. The flow is redirected and flattened into a film of liquid. The film leaves the plate and breaks up into ligaments and droplets due to surface tension and viscous forces within the liquid, and the action of shear forces between the liquid film and the surrounding gas.

Splash-plate atomizers belong to the category known as impinging jet atomizers. Because of their widespread application, impinging jet atomizers have been extensively investigated. Detailed theoretical studies of these atomizers were initiated by Hagerty and Shea [1] and Dixon et al. [2]. Later, Dombrowski and coworkers [3–6], in a number of studies, presented analytical models of droplet formation in thinning liquid films. Their model of this process provides a quantitative relationship between liquid properties, operating parameters, and the resulting droplet size. Huang [7] and Donaldson and Snedecker [8] also contributed to the understanding of the physics of atomization in these nozzles. Liquid film disintegration and atomization has been investigated by many researchers using experiments or theoretical analysis. On the experimental side, one can refer to Mansour and Chigier [9, 10], who conducted elaborate experiments to study the development, stability, and disintegration of liquid films issuing from a two-dimensional air-assisted nozzle. They found that the effect of introducing air in the nozzle is similar to the effect of inducing forced vibrations on the nozzle body. On the theoretical side, the study of Sirignano and coworkers [11, 12] provides detailed analysis of liquid film disintegration.

Splash-plate atomizers are widely used in chemical recovery boilers where black liquor from wood pulp is burned to recover pulping chemicals and produce steam. Black liquor droplet size is an important parameter for proper combustion. Droplets that are too large do not have sufficient time to dry and partially pyrolyze before reaching the char bed or walls, causing bed instability and possibly a blackout. Droplets that are too fine are entrained with the flue gas. This carryover can deposit on the upper furnace tubes, potentially plugging the flue gas passage. To better understand the performance of a particular nozzle, determination of the droplet size distribution is critical. This particle size distribution is usually determined by physical experimentation in a spray booth, using either black liquor or corn syrup. Droplet diameter is difficult to measure in situ. Therefore, although the generally ac-

cepted optimum droplet mass median diameter is approximately 3 mm [13], this has not been validated by extensive field testing.

On the particular application of splash-plate nozzles for chemical recovery boilers, many experimental and theoretical studies are available in the literature [13–19]. These studies have led to a general understanding of the flow and atomization characteristics of black liquor splash-plate nozzles. Bennington and Kerekes [14] used a small-scale splash-plate nozzle to study atomization in these nozzles.

Splash-plate atomizers are designed based on experimental measurements. Because of the complexity of the flow existing in these systems, there is no accurate technique that can relate the nozzle design to the spray droplet size and velocity distributions. Most spray nozzles are tested in ambient conditions and may not provide the same results under actual operating conditions. A computer code that could accurately predict spray flow characteristics and droplet size distribution based on specified operating conditions and nozzle configuration would be invaluable. From a practical point of view, such a computer code could be used for the following: to design an improved nozzle by investigating the effects of shape changes on spray characteristics; to predict flow and droplet size distribution of a specific nozzle or, conversely, to determine the optimum nozzle for a specific operation; and to provide input into computational fluid dynamics (CFD) models that solve the spray combustion to improve predictions of burnout, carryover, and combustion characteristics, resulting in a better assessment of the effects of fuel changes on the operation of the recovery boiler.

A computer code called *BLSpray* (black liquor Spray) has been developed to predict the liquid film characteristics of a splash-plate atomizer. It is believed that *BLSpray* is the first numerical simulation to address splash-plate atomization. The code predicts the liquid film thickness and velocity distributions, the pattern of film breakup, and the droplet size distribution for a splash-plate nozzle as a function of nozzle geometry and its operating conditions. A 3D numerical model was used that combines the solution of Navier–Stokes equations with an algorithm for tracking the liquid free surface in the presence of an arbitrary obstacle shape in the computational domain. This paper describes the numerical techniques used, validation of the model with available experimental measurements, and extensive numerical results for splash-plate atomizers. The paper includes simulation results on typical splash-plate nozzle designs from ALSTOM and Babcock & Wilcox under a wide range of operating conditions. The model used in *BLSpray* code was validated against two sets of experiments found in the literature, one for the spray droplet sizes during normal impingement of a water jet on

a plate, and the other for the film thickness and velocity distributions in a typical splash-plate nozzle.

Extensive simulations performed in the course of this study, and presented in this paper, cover detailed investigations on the influence of the nozzle geometrical design and operating conditions on the liquid film formation and breakup. The considered parameters include nozzle velocity, nozzle angle, liquid jet diameter, and liquid viscosity. One section of the paper is dedicated to showing the capability of *BLSpray* code in a complete flow simulation of a splash-plate nozzle, from film thickness and velocity evaluation up to the film breakup and droplet formation. By performing such a simulation on a typical ALSTOM nozzle design, droplet size distributions in the atomization zones were obtained at different angles from the splash-plate centerline.

In this paper, correlations for spray characterization of splash-plate atomizers are also discussed. These correlations provide mathematical formulations that relate the spray mean drop sizes to the liquid properties and liquid film characteristics at the nozzle exit. Correlations were obtained by running many different numerical simulations on typical splash-plate nozzles using *BLSpray* code.

NUMERICAL METHODS

Fluid Flow

This section briefly describes the mathematical formulations and computational procedures used in *BLSpray* code. The developed 3D numerical model of free surface flows is an Eulerian fixed-grid algorithm that utilizes a volume tracking approach to track fluid deformation. The flow governing equations assuming an incompressible, Newtonian, and laminar flow are

$$\nabla \cdot \mathbf{V} = 0 \tag{1}$$

$$\frac{\partial \mathbf{V}}{\partial t} + \nabla \cdot (\mathbf{V}\,\mathbf{V}) = -\frac{1}{\rho}\nabla p + \upsilon \nabla^2 \mathbf{V} + \frac{1}{\rho}\mathbf{F}_b \tag{2}$$

where $\mathbf{V}$ represents the velocity vector, p the pressure, ρ the density, υ the kinematic viscosity, and $\mathbf{F}_b$ any body forces (per unit volume) acting on the fluid. The assumption of laminar flow for the problem under consideration is reasonable. Assuming the internal flow through the splash-plate nozzle pipe (for black liquor as liquid with a high viscosity), the Reynolds number was

estimated to be around 2000, which is less than the critical Reynolds number corresponding to the onset of turbulence. Flow boundary conditions are required along both the computational grid and the liquid free surface. For splash-plate simulations, all grid boundaries are set as an *outflow* continuous boundary, except at the liquid jet inlet grids where an *inflow* continuous boundary is set. To reduce the computational time, the planar symmetries of the cases considered were exploited. At all symmetry planes, therefore, a *free-slip* boundary condition is used. It should be noted that the splash-plate interface is an internal boundary and not a grid boundary; at this interface a *no-slip* condition is applied.

For cells located on the liquid free surface, velocity boundary conditions are applied by requiring that the divergence of the velocity field be zero. Also across the interface, Laplace's equation specifies the surface-tension-induced jump in the normal stress p_s as

$$p_s = \gamma\kappa \tag{3}$$

where γ represents the liquid–gas surface tension and κ the total curvature of the interface.

A 3D fixed-grid Eulerian method was written specifically for free surface flows with surface tension. Equations (1) and (2) are discretized according to typical finite volume conventions on a rectilinear grid encompassing both the volume occupied by the jet and splash-plate prior to impact as well as sufficient volume to accommodate the subsequent liquid film deformation. Velocities and pressures are specified as on a traditional staggered grid: velocities at the center of cell faces and pressure at the cell center. The choice of a fixed-grid technique was made for several reasons: the relative simplicity of implementation; the capability of a volume tracking method to model gross fluid deformation, including breakup; and the relatively small demand on computational resources.

In addition to solving the flow equations within the liquid, the numerical model must also track the location of the liquid free surface. A well-known method for free surface tracking is that of Hirt and Nichols [20], initially introduced in the SOLA algorithm. In this study, however, a 3D volume tracking method called Youngs' algorithm [21] was used, which is a more sophisticated and accurate approach. The basis of this algorithm (as in [20]) is the "volume of fluid" technique, where a scalar function f is defined whose value is assumed to be unity when a cell is fully occupied by fluid and zero for an empty cell. Cells with values of $0 < f < 1$ contain a free sur-

face. Since function f is passively advected with the flow, f satisfies the advection equation

$$\frac{\partial f}{\partial t} + (\mathbf{V} \cdot \nabla) f = 0 \tag{4}$$

Note that function f with the above definition contains no information regarding the exact location of the interface. This is, in fact, the primary drawback of using volume tracking as an interface tracking method. On the other hand, volume tracking is relatively simple to implement even in three dimensions, retains this simplicity regardless of the complexity of the interface geometry, conserves mass (or volume, since the fluid is incompressible) exactly, and demands only a modest computational resource beyond that required by the flow solver. Given the volumetric nature of f and in order to maintain a sharp interface, the discretization of Eq. (4) requires special treatment. As with most other volume tracking algorithms, Youngs' algorithm [21] consists of two steps: an approximate reconstruction of the interface followed by a geometrical evaluation of volume fluxes across cell faces. The interface is reconstructed by locating a plane within each interface cell, corresponding exactly to the volume fraction f and to an estimate of the orientation of the interface, specified as a unit normal vector $\hat{n}$ directed into the liquid phase. In two dimensions, such an interface is simply a line crossing a cell. In three dimensions, the interface lines become three- to six-sided polygons, depending on how the plane slices the cell. Surface tension is modeled as a volume force acting on fluid near the free surface; the method used is the continuum surface force (CSF) model integrated with smoothed values of function f in evaluating free surface curvature.

Details of the fluid flow model, including the free surface advection using Youngs' algorithm and CSF model, are given by Bussmann et al. [22].

Nozzle Body

The body of the splash-plate nozzle in the computational domain is an internal obstacle that affects the fluid flow. The internal obstacles are treated in a manner similar to the volume of fluid method for free surface advection. Here, a volume fraction is defined as function Θ whose value is equal to one in the fluid and zero in the obstacle. The obstacle is characterized as a fluid of infinite density and zero velocity. The definition of Θ differs from that of the function f in that for liquid flow with a free surface, f is the fraction of a cell volume occupied by liquid, while Θ is the fraction of a cell volume occupied by both liquid and gas. The model does not solve for the

gas phase directly; therefore, the void volume replaces the gas volume of a cell. For a cell (i,j,k) of volume $v_{i,j,k}$, the volume fraction Θ is defined as

$$\Theta_{i,jk} = \frac{1}{v_{i,j,k}} \int \Theta \, dv \tag{5}$$

With this definition, Θ is a perfect step function only when obstacle boundaries coincide with lines of the computational mesh. In general, however, obstacle boundaries arbitrarily snake through the mesh, cutting through cells. This gives rise to Θ values in the range $0 \le \Theta \le 1$, which is necessary to avoid a "stair-step" model of a curved interior obstacle boundary. Cells with a value of Θ satisfying $0 < \Theta < 1$ are termed "partial flow cells" because a portion Θ of their finite difference volume is open to flow and the remaining portion $(1 - \Theta)$ is occupied by an obstacle closed to flow. For partial flow cells, the continuity, momentum, and volume of fluid equations [Eqs. (1), (2), and (4)] are modified as [23]

$$\nabla (\Theta \cdot \mathbf{V}) = 0 \tag{6}$$

$$\frac{\partial (\Theta \mathbf{V})}{\partial t} + \nabla \cdot (\Theta \mathbf{V} \mathbf{V}) = -\frac{\Theta}{\rho} \nabla p + \Theta \upsilon \nabla^2 + \frac{\Theta}{\rho} \mathbf{F}_b \tag{7}$$

$$\frac{\partial f}{\partial t} + (\Theta \mathbf{V} \cdot \nabla) f = 0 \tag{8}$$

Away from the obstacle inside the fluid computational domain where $\Theta = 1$, Eqs. (6)–(8) are reduced to Eqs. (1), (2), and (4), respectively. And inside the obstacle where $\Theta = 0$ there will be no calculation. It is at the partial flow cells where $0 < \Theta < 1$ that the above equations require special treatment in the discretization of volume fraction Θ. Because of a staggered grid, it is necessary to have a volume fraction Θ at the cell center, and area fractions Θ_x, Θ_y, and Θ_z at the cell faces in the x, y, and z directions, respectively. Boundary conditions that must be imposed on the liquid–obstacle interface are velocity boundary conditions. No-slip conditions on this interface are applied by defining "fictitious" velocities within obstacle cells adjacent to fluid cells. Velocities at the faces of these cells are set such that normal and tangential velocities at the liquid–obstacle interface become zero (no-slip condition). Details of the computational treatment of internal obstacles are given elsewhere [24] and will not be repeated here.

The fluid flow equations are solved on a Eulerian, rectangular, staggered mesh in a 3D Cartesian coordinate system. The computational domain encompasses the volume of the splash-plate nozzle and sufficient volume to cover liquid film deformation and breakup after exiting the nozzle. The mesh size was determined on the basis of a mesh refinement study in which the grid spacing was progressively decreased until further reductions made no significant changes in the predicted shape and thickness of the liquid film at the exit of the nozzle. The computational mesh considered for the simulations is uniform throughout the domain.

MODEL VALIDATION

The *BLSpray* code was validated against two sets of experiments found in the literature, one for the spray droplet sizes during normal impingement of a water jet on a plate, and the other for the film thickness and velocity distributions in a typical splash-plate nozzle.

The normal impact of a liquid jet on a solid plate. The first set of experiments is that of Ashgriz et al. [25] for a 0.45 mm diameter water jet impinging normally on a 1.35 mm diameter flat disc at different jet impact velocities ranging from 12 m/s to 26.8 m/s. *BLSpray* was used to simulate this experiment; Fig. 1 shows a close-up view of the simulation results at the drop formation stage. A comparison between the two cases presented in this figure shows that as the jet impinging velocity increases, the size of the droplets decreases. This is because the liquid disk formed as a result of the jet impact is thinner for a jet with a higher impact velocity, and droplets formed from the breakup of a thinner liquid film will have smaller sizes. A quantitative comparison between the numerical simulation and experimental results [25] is summarized in Table 1. The results of this initial validation show that the program accurately predicts the spray drop sizes.

The mean drop diameter given in Table 1 is $D[1,0]$, the sum of all diameters divided by the number of drops identified in the atomization zone, i.e., $\frac{1}{n}\sum_{1}^{n} d_i$ where d represents the drop diameter and n is the number of drops.

Simulation results show the disintegration mechanism of the liquid jet. As soon as the jet impacts on the plate, a liquid film is formed. As the film moves in the radial direction, it becomes thinner. Figure 1 shows formation of waves around the periphery of the liquid disk as soon as the liquid film leaves the plate. The propagation of these waves results in breakup of the

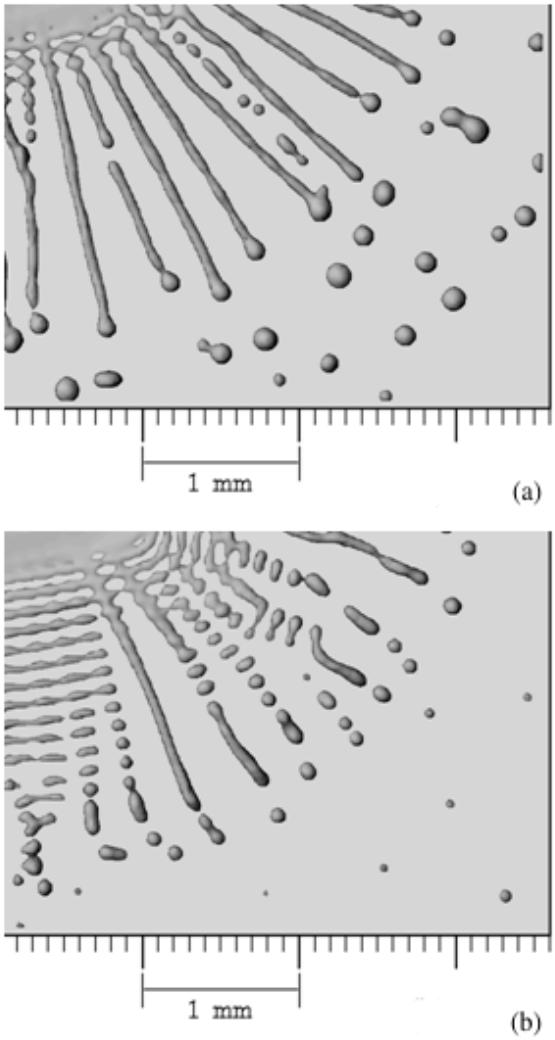

Fig. 1 Calculated top view images of (a) the 12 m/s and (b) the 26.8 m/s impact of a 0.45 mm diameter water jet on a 1.35 mm diam splash-plate. The images show the liquid film and spray at the drop formation stage.

Table 1 Quantitative Validation of *BLSpray* with Measurements of Ashgriz et al. [25]

Jet velocity, m/s	12	26.8
Measured mean drop diameter, μm	~160	~80
Range of drop diameter in simulation, μm	100–200	50–100
Diameter of majority of drops in simulation, μm	~150	~80

liquid disk into small liquid ligaments, which, in turn break up to form small droplets. As seen in Fig. 1, the liquid film breakup into ligaments appears as straight lines directed outward from the film periphery (finger formation). This phenomenon has been observed in experiments as well. Azuma and Wakimoto [26] provided many experimental photographs that show a similar feature for a high-speed jet impact.

Black liquor sheet thickness and velocity at the tip of a splash-plate. The second set of experimental results is for the liquid film characteristics at the tip of a typical splash-plate nozzle. In the *BLSpray* code, the nozzle configuration eventually progressed from a flat plate to a complex full nozzle body. In 1989, Obuskovic and Adams [27] performed experiments in a laboratory to study the spray characteristics of corn syrup. Since the properties of corn syrup at room temperature are similar to those of black liquor at firing temperature, the spray characteristics of corn syrup were studied. These experiments were carried out at two different viscosities: 175 and 325 mPa·s. Obuskovic and Adams [27] measured the sheet thickness and velocity at the tip of the nozzle. The splash-plate nozzle considered in the experiments was a typical Babcock & Wilcox splash-plate nozzle for which the nozzle diameter was 11.9 mm, nozzle velocity 7.1 m/s, and nozzle angle 52°. The *BLSpray* code was used to simulate this experiment; the same liquid properties and nozzle configuration were used in both the theoretical and experi-

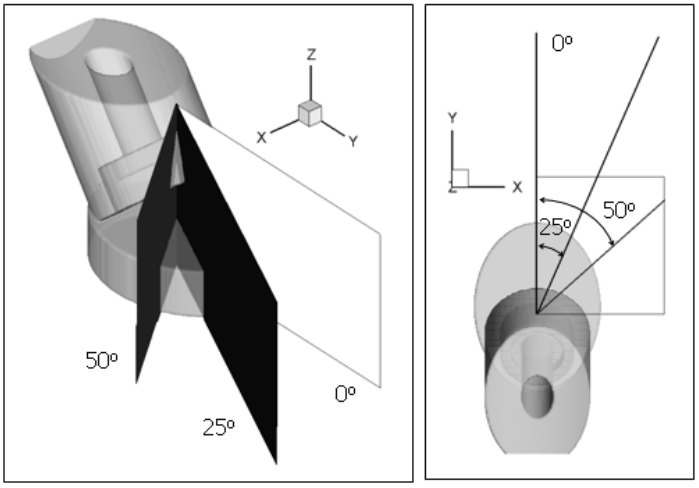

Fig. 2 The splash-plate nozzle considered for model validation and the three different angles from the plate centerline along with their corresponding cross-sectional planes. Comparison between the results of simulation with available experimental measurements [27] was performed on these cross sections.

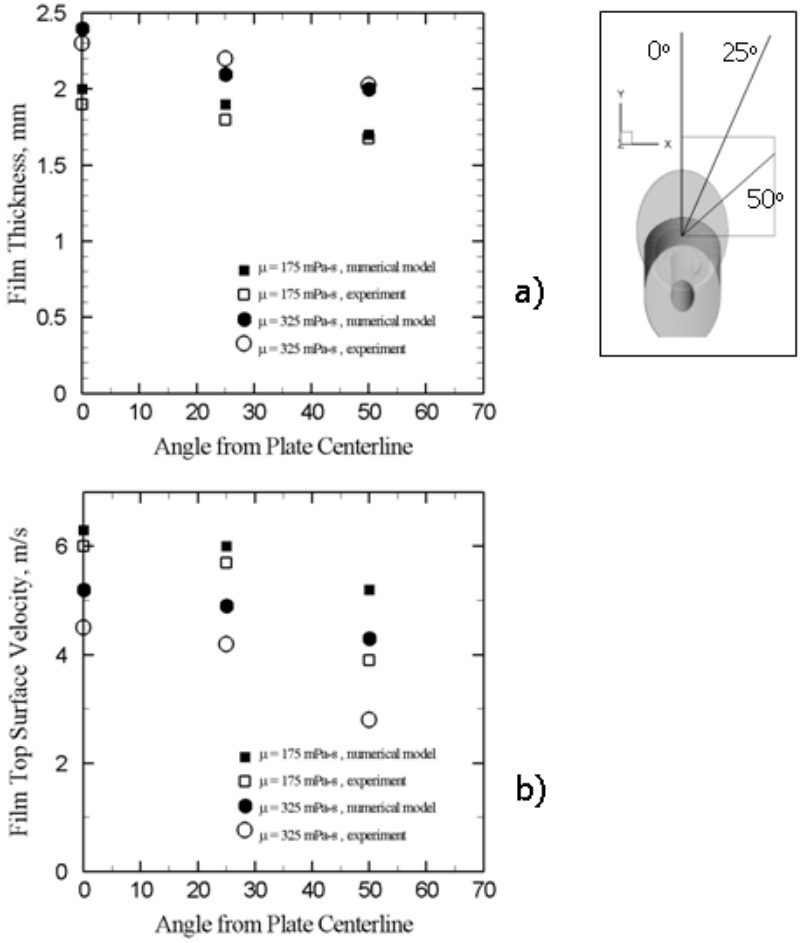

Fig. 3 Comparison between the numerical results of the *BLSpray* code with available experimental measurements [27] for a typical splash-plate nozzle at two different viscosities. The results are compared for (a) the film thickness, and (b) the film top surface velocity against the angle from the plate centerline. The nozzle velocity was 7.1 m/s.

mental runs. Figure 2 shows the shape of the splash-plate nozzle and the three angles from the plate centerline at which the numerical results and measurements were compared with each other. Figure 3 summarizes the results from simulation and measurements for both sets of viscosities. This figure shows a detailed quantitative comparison between the results of simulations and experimental measurements. The sheet thickness and velocity at different angles from the plate centerline were obtained from simulations and

compared to measured values. As observed in Fig. 3a, both simulations and experiments show that for the case with higher viscosity, the liquid film is thicker. When the viscosity is increased, more liquid momentum is lost due to viscous dissipation; therefore, the velocity of the sheet at the rim of the splash-plate is decreased (Fig. 3b). Since the nozzle flow rate (and inlet velocity) for both viscosity cases is equal, the film for the more viscous liquid will be thicker (Fig. 3a). For both cases, the film thickness and velocity are decreased (Fig. 3) at a higher angle from the plate centerline. This is because the liquid jet impacts the plate with an angle (52°, in this case); therefore, more liquid flows close to the centerline. At a normal (90°) impingement of a liquid jet on a plate, film thickness and velocity will be uniform in the angular direction.

Comparisons between numerical simulations and experimental measurements show that there is close agreement between the two results for the film thickness in both cases of low and high viscosities. The difference is less than 5% (Fig. 3a). For the film top surface velocity, there is good agreement at the angles close to the plate centerline. The difference is less than 5% for the case with lower viscosity, and 14% for the case with higher viscosity (Fig. 3b). There are, however, discrepancies between the two results for the top surface velocity at higher angles from the plate centerline. For example, at the 50° angle from the plate centerline, the discrepancy between the calculated and measured velocities is around 25% for the lower viscosity and 35% for the higher viscosity (Fig. 3b). This discrepancy may be attributed to the uncertainties of the velocity measurements in the experiments [27], where the velocity of the random irregularities at the top surface of the film was measured and assumed to be the same as the film velocity. Moreover, as mentioned in [27], when measuring velocities, the alignment of the fiber-optic probes with the direction of the flow is important. Any misalignment can change the measured velocity significantly. The importance of the alignment in the flow direction is more pronounced at higher angles from the plate centerline. The uncertainties of velocity measurements at higher angles can be seen in Fig. 3 (or more clearly in Figs. 5 and 6 of [27]). While the measured film thickness changes smoothly with the angle from the centerline, the measured top surface velocity has a sudden change after an angle of 25°.

In summary, the comparison performed in this section between numerical results and experimental measurements [25, 27] demonstrates the accuracy of the numerical model used in *BLSpray* code in predicting the film thickness and its velocity distributions, and spray drop sizes for splash-plate nozzles. The model, therefore, can be used to predict the film characteristics

behavior of a flow into a nozzle at different inlet liquid conditions, and also as a tool in the design of new nozzles.

DROPLET SIZE DISTRIBUTION

The numerical simulation of a liquid film to the breakup point, and formation of droplets and spray, can be achieved by using a large computational domain. To resolve a thin liquid film before breakup, the computa- tional mesh needs to be sufficiently fine. As a result, to obtain droplet sizes of a spray directly from numerical simulation, one has to devote a large amount of computational time and effort proportional to the size of the domain and computational mesh. To overcome the requirement for the large amount of CPU time needed to run a simulation, *BLSpray* is facilitated with a special feature that can accommodate different simulation blocks. Using this feature, the large computational domain is broken into a number of smaller domains or blocks. When the film shape in a computational block reaches a steady-state condition, the simulation is terminated and all the flow information (velocity, pressure, and volume fraction) are stored in a specific file. This file is then read in the next simulation step that continues in an adjacent block. Any number of blocks is permitted and blocks can be of different sizes. Computational time and effort for a simulation depends on the number of blocks used to reach the formation of droplets. This paper will discuss numerical results for flow simulations in a typical ALSTOM splash-plate nozzle that continued until droplets were formed. Droplet size distribution was obtained directly from the results of the model. The simulation conditions were as follows.

Typical ALSTOM nozzle:	32 mm bore
	45° nozzle angle
	4 m/s nozzle velocity
Fluid:	black liquor
	viscosity 200 mPa·s
	density 1350 kg/m^3
	surface tension 60 mN/m

Images of the flow simulation in the nozzle at different times after the start of the flow into the nozzle are shown in Fig. 4. This figure also shows the shape of the splash-plate, which is fully closed in the back with a smooth transition from the pipe to the splash-plate. When the black liquor jet

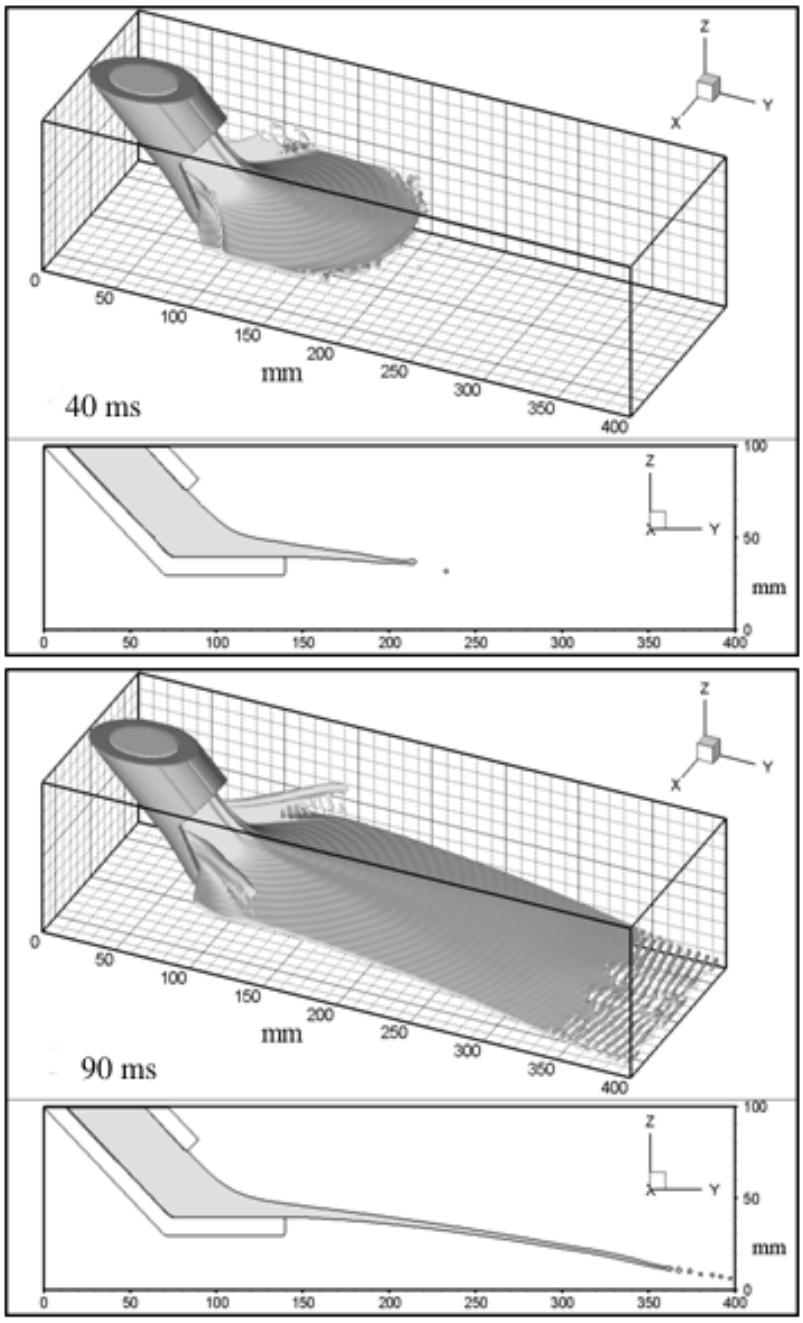

Fig. 4 3D view and centerline cross section of the evolution of black liquor flow into a typical ALSTOM splash-plate nozzle. This figure shows formation of a liquid sheet, and its breakup into ligaments and droplets.

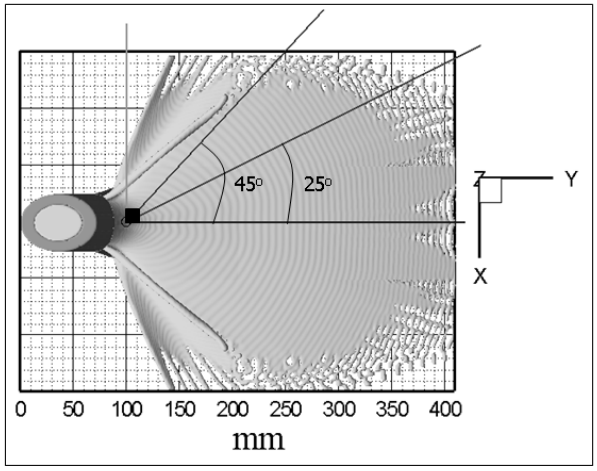

Fig. 5 Top view of the liquid film for flow simulation in a typical ALSTOM splash-plate nozzle showing the breakup length at different angles from the plate centerline.

impacts on the splash-plate, it makes a thin liquid film spreading to the front and the two sides of the plate. Wave formation on the liquid film breaks it up shortly after the film leaves the plate. An important aspect in the design of a splash-plate nozzle is the way it diverts the backward flow toward the main part of the liquid film. The backward flow is the liquid that flows in the opposite direction of the spray. The diverted backward flow for the nozzle under consideration is clearly seen in Fig. 4 as liquid sheets at the two sides of the splash-plate edges (known as side skirts). These side skirts have thick rims at the top; although the sheets break up into small droplets, the thick rims remain intact and continue flowing like liquid jets.

The film breakup length and pattern for the nozzle can be seen more clearly in Fig. 5, where a top view of the liquid film covering a larger domain is presented. From this figure, the film breakup length at different angles from the plate centerline can be calculated, as shown for $\theta = 25^\circ$ and $\theta = 45^\circ$. The result of this calculation is given in Fig. 6, where the variation of the film breakup length against the angle from the plate centerline is plotted. It should be noted that the film breakup length depends on many factors, one of which is the nozzle angle. For this simulation, the nozzle angle was 45°. When the nozzle angle is increased, the rate of film breakup length variation against the angle from the plate centerline will decrease, e.g., for a jet normal to a plate (nozzle angle of 90°), the film breakup length will be the same for all angles on the plate.

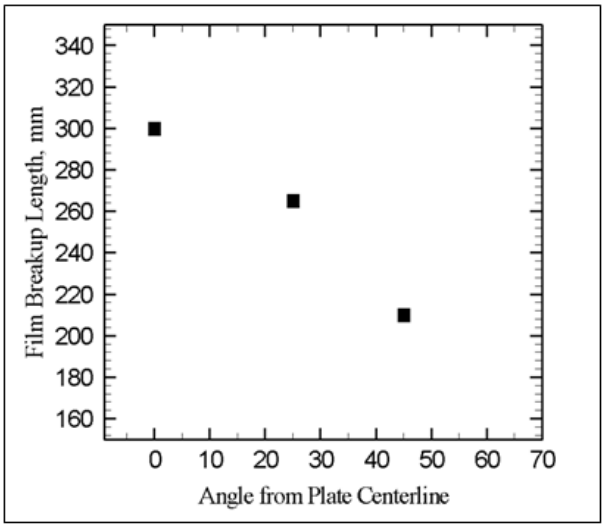

Fig. 6 Variation of the film breakup length against angle from the plate centerline for flow simulation in a typical ALSTOM splash-plate nozzle.

From the simulation results, all information regarding the flow, such as velocity and pressure, over the entire computational domain is known. The complete film thickness and velocity distributions around the splash-plate and up to the breakup zone can be obtained from these results. In this case, the parameter of interest is the droplet size distribution. Figure 7 shows images of the full simulation at the point where the final droplets are forming. Figures 7a and 7b depict the atomization zones close to the plate centerline (between $\theta = 0^\circ$ and $\theta = 10^\circ$) and on the side of the nozzle (between $\theta = 25^\circ$ and $\theta = 45^\circ$), respectively.

In order to analyze the droplet size from simulation results, the original data file from the calculation is used to give the size and position of all droplets in a desired computational domain. The shape of a liquid volume will eventually change to a sphere because of surface tension. Therefore, the diameter of each droplet is determined based on the calculated volume and assuming a spherical shape. The results of the program for the two atomization zones (Figs. 7a and 7b) are as follows. For a small area of the atomization zone close to the plate centerline (between $\theta = 0^\circ$ and $\theta = 10^\circ$ from the plate centerline, Fig. 7a), a total number of 51 droplets, excluding the symmetric part (or 102 droplets for the whole domain), were identified. Most droplets had a size that ranged from 4 to 8 mm in diameter. The average diameter size was 6.16 mm. Figure 8a shows the diameter of identified droplets and

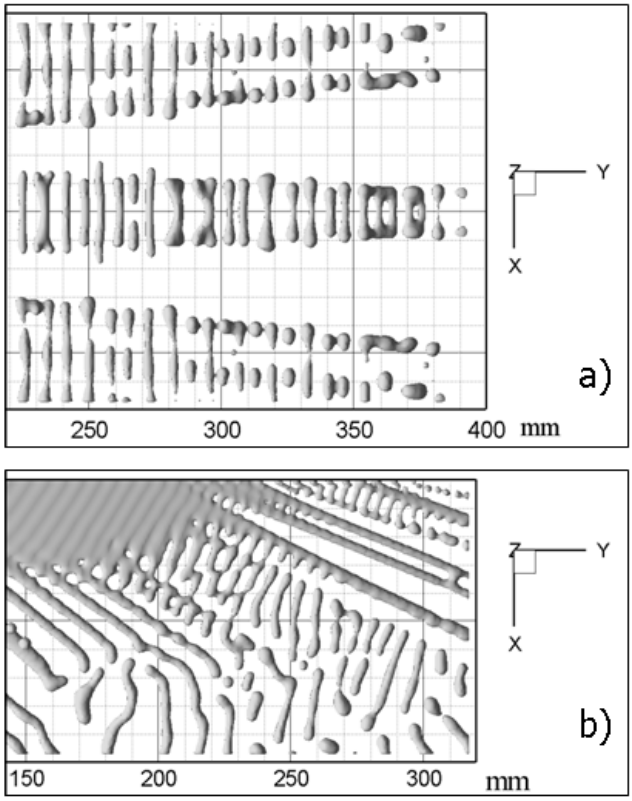

Fig. 7 Top close-up view of the atomization zone showing the size and position of droplets formed: (a) close to the plate centerline (between $\theta = 0^\circ$ and $\theta = 10^\circ$ from the plate centerline) and (b) in the side of the nozzle (between $\theta = 25^\circ$ and $\theta = 45^\circ$).

their average value in the first atomization zone. For the atomization zone on the side of the nozzle (between $\theta = 25^\circ$ and $\theta = 45^\circ$ from the plate centerline, Fig. 7b), a total number of 16 droplets, with size ranging from 3 to 7 mm in diameter, were identified. Figure 8b shows the diameter of identified droplets and their average value (5.43 mm) in the second atomization zone.

A droplet size distribution analysis was performed based on the number of droplets in each size range for the two atomization zones. The results are given in Fig. 9, where droplet number density is plotted against droplet diameter. Figure 9a corresponds to the first atomization zone, the domain shown in Fig. 7a (between $\theta = 0^\circ$ and $\theta = 10^\circ$, for which droplet sizes were given in Fig. 8a). Figure 9b corresponds to the second atomization zone, the domain shown in Fig. 7b (between $\theta = 25^\circ$ and $\theta = 45^\circ$, for which droplet

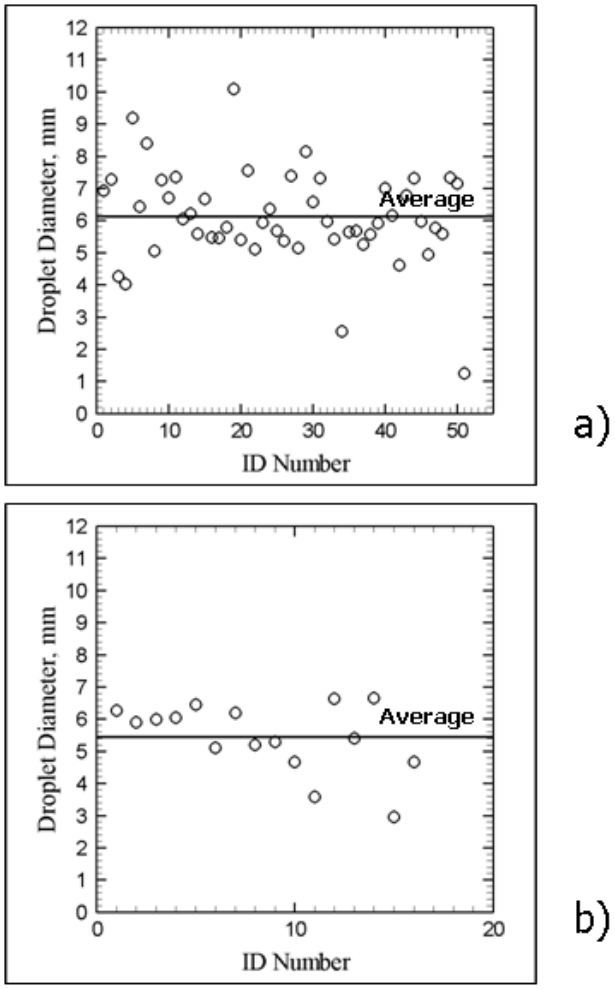

Fig. 8 Diameter of droplets identified in a small portion of the simulated atomization zones: (a) close to the plate centerline (between $\theta = 0^\circ$ and $\theta = 10^\circ$ from the plate centerline) and (b) in the side of the nozzle (between $\theta = 25^\circ$ and $\theta = 45^\circ$).

sizes were given in Fig. 8b). These figures indicate a normal droplet size distribution for both atomization zones. The main part of the spray in both zones consists of droplets 5, 6, and 7 mm in diameter. For the zone close to the plate centerline, 22% of droplets have a diameter of 5 mm, 33% have a diameter of 6 mm, and 27% have a diameter of 7 mm (Fig. 9a). For the side zone, 38% of droplets have a diameter of 5 mm, 38% have a diameter of 6 mm, and 12% have a diameter of 7 mm (Fig. 9b). It should be noted

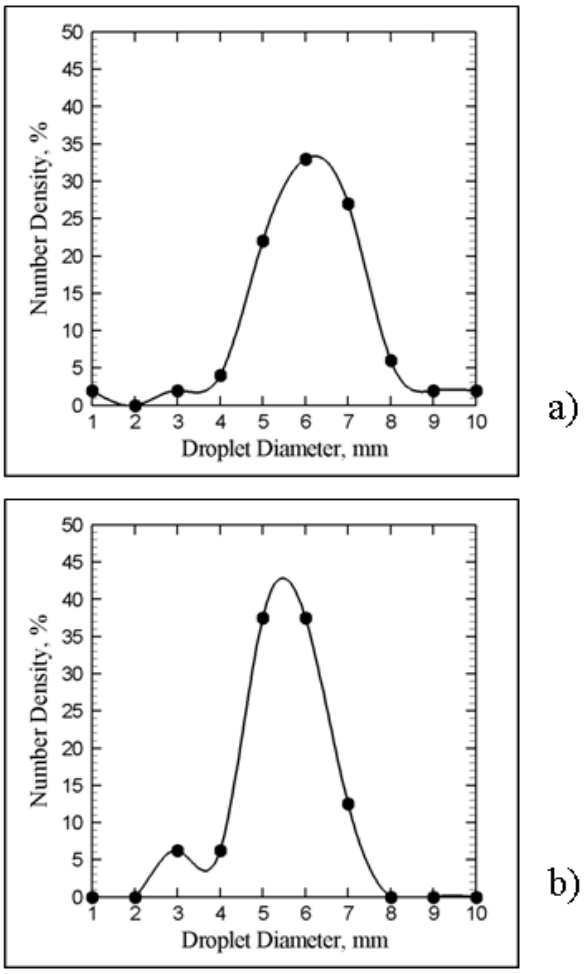

Fig. 9 Droplet size distribution for droplets identified in a small portion of the simulated atomization zones: (a) close to the plate centerline (between $\theta = 0^\circ$ and $\theta = 10^\circ$ from the plate centerline), and (b) in the side of the nozzle (between $\theta = 25^\circ$ and $\theta = 45^\circ$).

that the droplet size distributions given in Fig. 9 correspond to the two atomization zones depicted at a certain time and locations around the nozzle (Fig. 7). The droplet sizes obtained for these sample zones resolve the whole spray characteristics for the following reasons. First, all the simulations were run to the steady-state condition and, therefore, the results are independent of time. Second, other atomization zones at different times and locations were also tested to verify the presented spray size distributions.

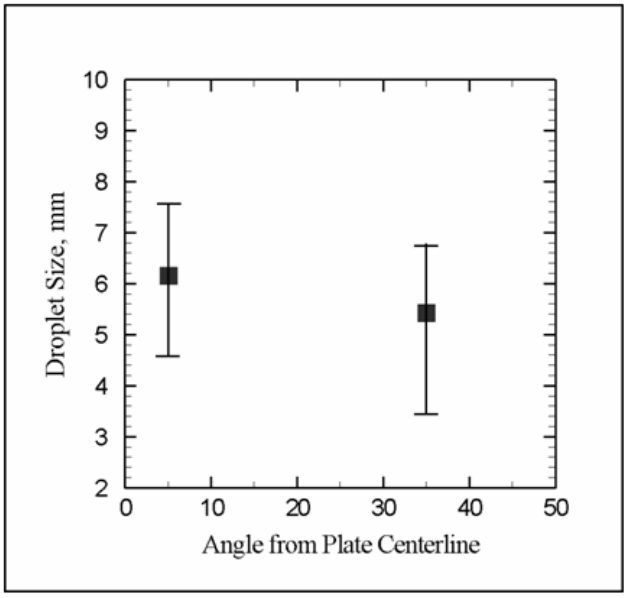

Fig. 10 Droplet size against the angle from the plate centerline for flow simulation in a typical ALSTOM splash-plate nozzle. Symbols correspond to the average droplet size; bars indicate the size range of 85% of the droplets in each case.

Based on the above figures and the position of the two atomization zones, droplet size can be plotted against angle from the plate centerline. This plot is shown in Fig. 10. As observed, the average droplet size is slightly decreased for higher angles from the plate centerline. The difference, however, is less than 12%. As a result, the average droplet size obtained close to the centerline is a good estimate of the average droplet size for spray angles up to $\theta = 45^{\circ}$. For angles from the plate centerline higher than 45°, liquid streaks, instead of liquid film, are formed, as seen in Fig. 5. These small liquid jets, along with the diverted backflow jets (seen in the same figure), will have a different breakup mechanism than that of the main spray.

The droplet size distributions presented in Fig. 9 are based on the number of droplets at each diameter range (number density). When the distributions are plotted for droplets' volumes (i.e., mass fraction), the distributions will have a lognormal shape rather than normal. To show this more clearly, the result of drop size distribution for the same ALSTOM nozzle from Fig. 4, but with assuming lower viscosity for black liquor that results in a wider range of drop sizes, is shown in Fig. 11. Figure 11 shows drop size distributions based on number density (Fig. 11a) and mass fraction (Fig. 11b) for

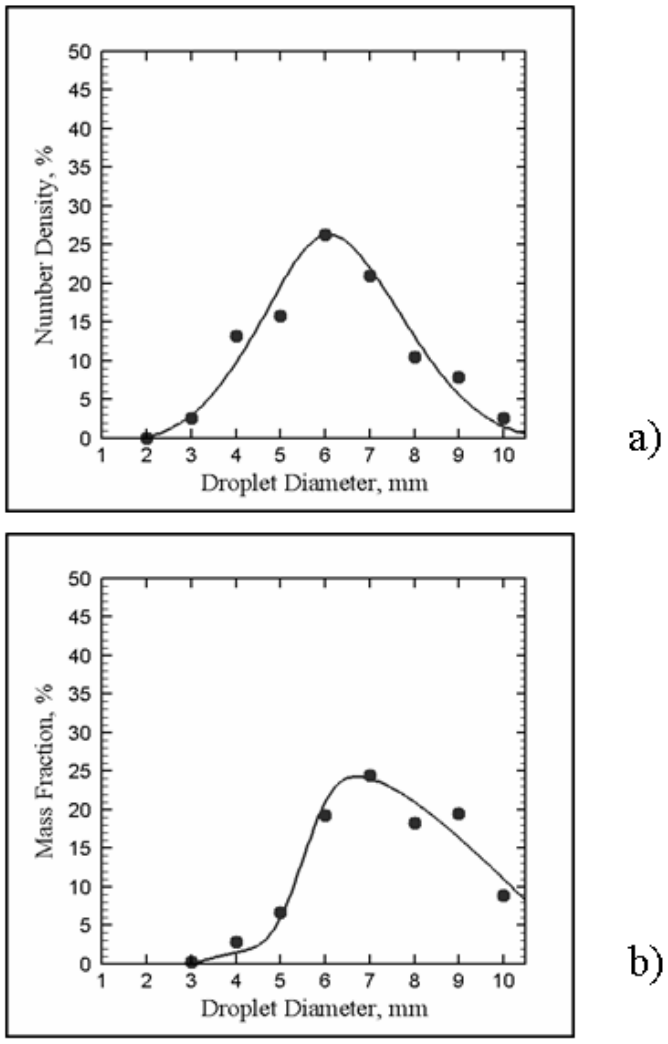

Fig. 11 Droplet size distribution for the ALSTOM splash-plate nozzle shown in Fig. 4 assuming a viscosity of 50 mPa·s for black liquor. The distribution is associated with the atomization zone close to the plate centerline (between $\theta = 0^\circ$ and $\theta = 10^\circ$ from the plate centerline) and is based on (a) number density and (b) mass fraction.

the same nozzle and operating conditions given in this section except for the viscosity, which has been reduced to 50 mPa·s. The distribution is associated with the atomization zone close to the plate centerline (between $\theta = 0^\circ$ and $\theta = 10^\circ$ from the plate centerline). From this figure, it can be seen that while

the drop size distribution based on number density has a normal shape, the distribution based on mass fraction is closer to lognormality.

The simulation results presented in detail in this section demonstrate the capability of the *BLSpray* code to complete a simulation of a splash-plate nozzle from the film thickness and velocity evaluation up to the film breakup and droplet formation. It should be mentioned that the numerical techniques considered in *BLSpray* did not consider secondary breakup. Therefore, the film and spray characterization presented here is based on film primary breakup. Flow disturbances were also not included in these simulations. The surface waves were formed due to the inherent instabilities and inhomogeneity in the liquid film velocities. Any disturbance in fluid flow will enhance the film breakup and will affect the breakup mechanism, spray pattern, and droplet size.

EFFECTS OF NOZZLE PARAMETERS

BLSpray is a useful tool for determining the effect of various parameters on the formation of liquid sheet and subsequent droplets. Important operating parameters that affect the shape of the liquid film and the resulting atomization and droplet size are the nozzle geometrical parameters, flow conditions, and liquid properties. In this section, the following parameters are tested:

- Nozzle diameter 12, 22, and 32 mm (0.5, 0.87, 1.25 in)
- Nozzle angle 35°, 45°, and 55°
- Nozzle velocity 5, 10, and 18 m/s

The effect of liquid viscosity was studied in the model validation section in this paper. The results were analyzed at three different angles from the plate centerline: $\theta = 0^\circ$, 45°, and 90°. The results of the simulations were compared with respect to sheet thickness and velocity at the tip of the plate. The following is a brief discussion of the simulations and corresponding results.

Nozzle Diameter. Three nozzles diameters were tested: 12, 22, and 32 mm. All other parameters, including nozzle velocity (10 m/s) and nozzle angle (45°), were held constant. The results of simulations for these cases are given in Fig. 12. Figure 12a shows the film thickness at the tip of the splash-plate, while Fig. 12b shows the corresponding top surface velocity against the angle from the plate centerline. The film thickness increased in all directions with increasing nozzle diameter (Fig. 12a). This was expected since the flow rate increases as the nozzle diameter increases (nozzle velocity is held constant at 10 m/s). The sheet breaks up at a distance further

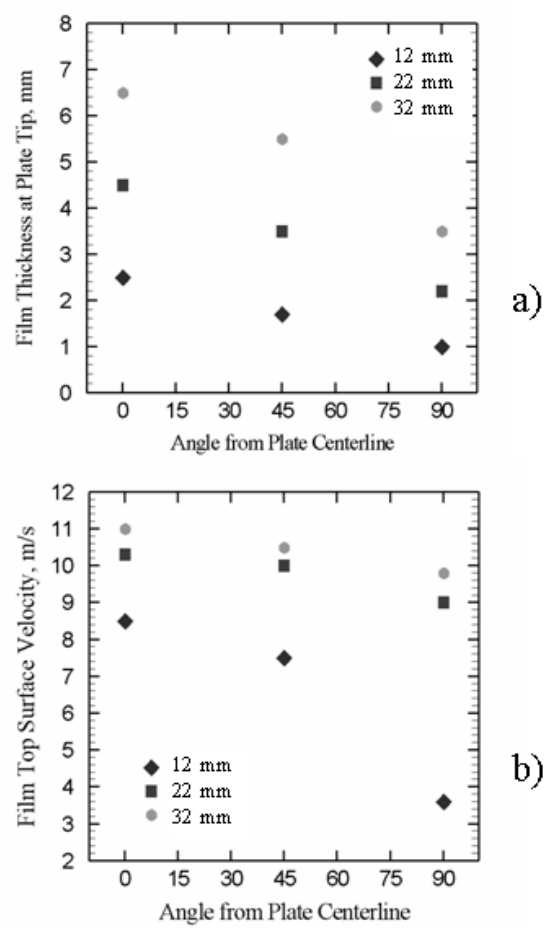

Fig. 12 The effects of nozzle diameter on (a) the liquid film thickness and (b) the film top surface velocity at the tip of the splash-plate nozzle. The nozzle diameters were 12, 22, and 32 mm. For all cases, the nozzle velocity was 10 m/s and nozzle angle was 45°.

from the plate as the nozzle diameter increases. As the liquid film leaves the plate, the velocity direction at the plate tip is nearly parallel to the plate at all cross sections. The top surface velocity is significantly lower for the smallest diameter than the other two cases (Fig. 12b). This is because most of the liquid kinetic energy is lost due to viscous dissipation. As the nozzle diameter increases, the film thickness also increases, but the boundary layer thickness remains constant. As a result, the difference in the top surface velocity between the two larger diameters (22 and 32 mm) is less pronounced.

Nozzle Angle. Three nozzle angles were tested (35°, 45°, and 55°), with all other parameters, including nozzle velocity (10 m/s) and nozzle diameter (22 mm), remaining constant. Results, shown in Fig. 13, indicate that the effect of nozzle angle varies depending on the angle from the plate centerline. At $\theta = 0°$, for every 10° increase in nozzle angle, the film thickness decreases by nearly 20%. This indicates that for nozzles with higher angles,

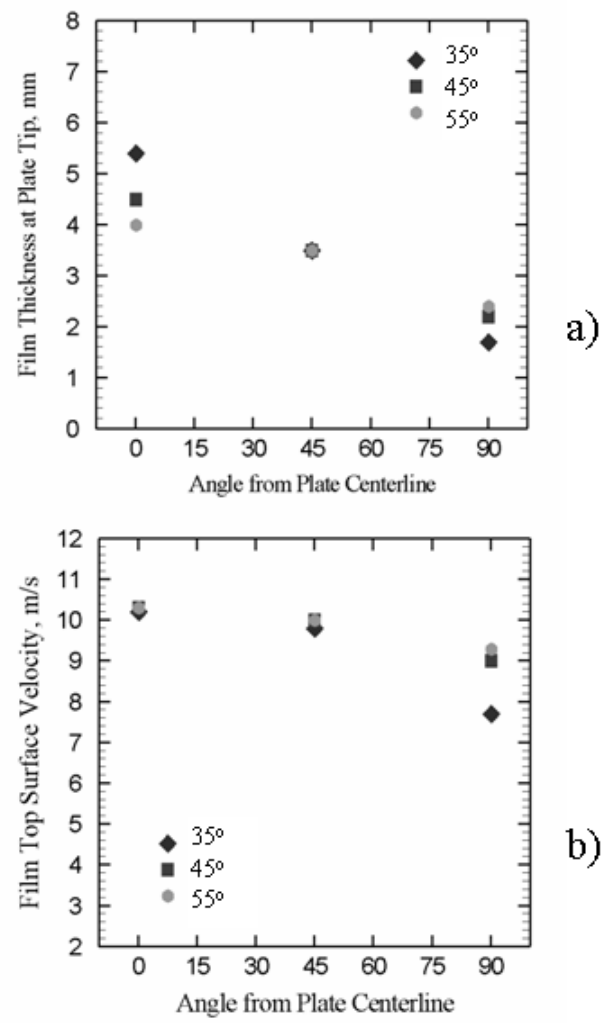

Fig. 13 The effects of nozzle angle on (a) the liquid film thickness and (b) the film top surface velocity at the tip of the splash-plate nozzle. The nozzle angles were 35°, 45°, and 55°. For all cases, the nozzle diameter was 22 mm and nozzle velocity was 10 m/s.

the atomization at the plate centerline occurs at a shorter distance from the splash-plate because the film thickness approaches the limit value for the breakup more rapidly. At $\theta = 45^\circ$, the effect of nozzle angle is negligible. The film thickness remains the same. At $\theta = 90^\circ$, the film thickness increases slightly as the nozzle angle increases. The film breaks up at a distance further from the splash-plate for the higher nozzle angle. At lower nozzle angles, the film thickness is thicker at the plane of symmetry ($\theta = 0^\circ$ cross section) and thinner at the cross section of $\theta = 90^\circ$. When the nozzle angle is increased, the film thickness along the plate tip becomes more uniform. Since the droplet size distribution is directly related to the film thickness and velocity distributions, it can be concluded that using a lower nozzle angle will result in a wider range of droplet sizes. Therefore, as the nozzle angle increases, more atomization occurs toward the sides of the splash-plate, and the atomization zone at the plane of symmetry ($\theta = 0^\circ$) will be closer to the splash-plate. The magnitude of the velocity at the splash-plate exit for all cases is close to the nozzle velocity.

Nozzle Velocity. Three nozzle velocities were tested (5, 10, and 18 m/s), with all other parameters, including nozzle diameter (22 mm) and nozzle angle (45°), remaining constant. The sheet thickness and velocity results are summarized in Fig. 14. As can be seen in Fig. 14a, the nozzle velocity has no effect on sheet thickness. Even at $\theta = 90^\circ$, there is only a very slight difference between the three cases. As the nozzle velocity increases, the velocity boundary layer thickness is decreased. This means that the effect of splash-plate deceleration of the jet flow is more significant at lower velocities. Because of the lower initial kinetic energy of the jet and higher percentage of energy loss due to viscous dissipation, the size of the atomized droplets are larger for jets with lower velocity. Figure 14b indicates that the rate of velocity change with respect to the angle from plate centerline is nearly the same for all cases.

An estimate of the film flow rate at different angles from the plate centerline can be obtained based on the thickness and velocity of the film at the point it leaves the splash-plate. The effects of nozzle diameter, nozzle angle, and nozzle velocity on the black liquor radial flow distribution were investigated. It was found that the nozzle diameter and nozzle velocity have no significant effect on the radial flow distribution. The effect of nozzle angle, however, was considerable; the results are summarized in Table 2.

As seen from this table, increasing the nozzle angle results in a more even distribution of flow and spray in the plane of the splash-plate nozzle. As the nozzle angle is decreased, the spray will be more concentrated toward the nozzle centerline.

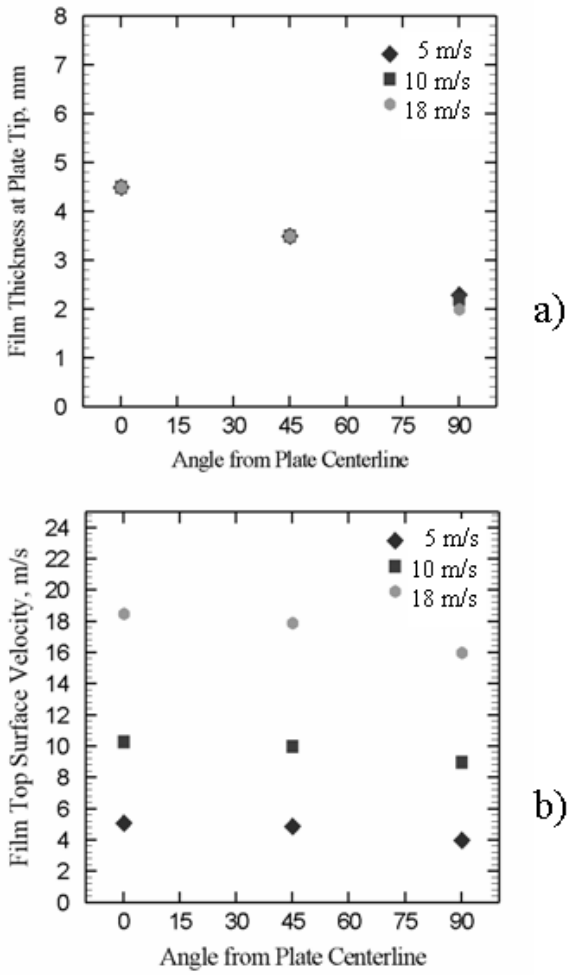

Fig. 14 The effects of nozzle velocity on (a) the liquid film thickness and (b) the film top surface velocity at the tip of the splash-plate nozzle. The nozzle velocities were 5, 10, and 18 m/s. For all cases, the nozzle diameter was 22 mm and nozzle angle was 45°.

Table 2 Effect of Nozzle Angle on Radial Spray Distribution

Nozzle angle	Radial flow distribution (%)		
	$\theta = 0^\circ$ to $\theta = 45^\circ$	$\theta = 45^\circ$ to $\theta = 90^\circ$	$\theta = 90^\circ$ to $\theta = 180^\circ$
35°	52	30	18
45°	45	35	20
55°	44	33	23

FILM AND SPRAY CHARACTERISTICS

Correlations for Mean Drop Size. As shown in the previous section, the *BLSpray* code can be used directly to simulate the liquid film at the exit of a splash-plate nozzle up to the breakup point and formation of drops and spray. There are, however, certain computational limitations. Numerical solutions for such fluid flow conditions can be achieved by using a large computational domain. Also, to resolve a thin liquid film before breakup, the computational mesh needs to be sufficiently fine. As a result, to obtain drop size distribution of a spray directly from *BLSpray*, one has to devote a large amount of computational time and effort proportional to the size of the domain and computational mesh. A practical approach to obtain spray drop sizes from the *BLSpray* code is to run simulations for a nozzle shape and operating conditions in order to get the film thickness and velocity distributions at different angles from the plate centerline. Proper formulations are then used to correlate the thickness and velocity at each angle (close to the plate tip) to the corresponding mean drop size at that angle. Such correlations were developed between black liquor film characteristics at the nozzle exit and the spray mean drop sizes. This was done by running many different numerical simulations on typical splash-plate nozzles using *BLSpray* code. First, a close inspection of the numerical results was performed to extract all information regarding the liquid film and spray. Second, the important parameters that affect the drop size were identified and their individual effects were formulated. Finally, a formula that correlates these parameters was developed, namely, black liquor properties and liquid film characteristics to the spray mean drop sizes.

When the film thickness and velocity close to the tip of the splash-plate is correlated to the droplet size, the *BLSpray* code can be run to simulate the flow into the nozzle using a small computational domain that extends slightly further than the boundaries of the nozzle body. The simulation is terminated when the film shape reaches a steady-state condition, and the film thickness and velocity distributions at the plane of the liquid film are obtained from numerical results. These values are then used in the correlation to obtain the eventual droplet size distribution of the spray.

To obtain correlations, many different cases were run on a typical ALSTOM splash-plate nozzle similar to the nozzle shown in Fig. 4. These cases covered a wide range of liquid properties and nozzle velocity. Liquid viscosity ranged from 50 to 1000 cP (*centi Poise* equal to mPa·s), surface tension from 30 to 120 mN/m, and density from 700 to 2000 kg/m^3. Nozzle velocity ranged from 1 to 10 m/s. Mesh size for all cases was based on one cell per

one millimeter. The mesh size was determined on the basis of a mesh refinement study in which the grid spacing was progressively decreased until further reductions made no significant changes in the predicted shape, thickness, and velocity of the liquid film at the exit of the nozzle. The gravity for all cases was in the direction normal to the top surface of the splash-plate. In order to study the film characteristics and find a correlation for drop size, film and spray characteristics data was extracted from numerical results. The information extracted included film thickness and velocity distributions at the nozzle exit at each angle from the plate centerline and the mean drop diameter at the corresponding angle.

Figure 15 shows the effects of liquid properties (here, black liquor) and nozzle velocity on mean drop size for the ALSTOM nozzle under consideration. The results show that when the viscosity is increased, the liquid ligaments remain as ligaments for a longer period of time before breaking up into droplets. The formation of droplets is therefore delayed, and the resulting droplets are larger in size. Surface tension has a significant effect on mean droplet size. When the surface tension is increased, the mean droplet size is increased substantially. This is because at a higher surface tension, many ligaments do not break up and form large single droplets. When the liquor density is increased, the mean droplet size is decreased due to higher momentum, and thus higher kinetic energy, of the liquid prior to impact. When the nozzle velocity is increased, the film thickness at the film breakup point is reduced. The resulting mean droplet size is decreased.

By performing a power-fit curve fitting on the effect of individual parameters shown in Fig. 15, a formula was developed that correlates the spray mean drop diameter to the liquid properties and nozzle velocity. For all these simulation cases, one specific splash-plate nozzle (similar to Fig. 4), with a set nozzle diameter and nozzle angle, was used. Therefore, another formula was obtained that correlates the spray drop sizes to the film characteristics (i.e., film thickness and velocity at the nozzle exit) instead of nozzle parameters. The developed formula can be applied to any splash-plate nozzle as long as the film thickness and velocity distributions at the exit of the nozzle are known. An error analysis for the correlation was performed by comparing the estimates calculated from the correlation with those obtained form the simulation using the *BLSpray* code. The results of the correlation were found to be good estimations for the drop size. The error for most cases was less than 5%.

Having developed the correlations, one can run the *BLSpray* computer code for a small computational domain that extends slightly farther than the exit plane of the nozzle. At the end of a simulation, the film thickness and

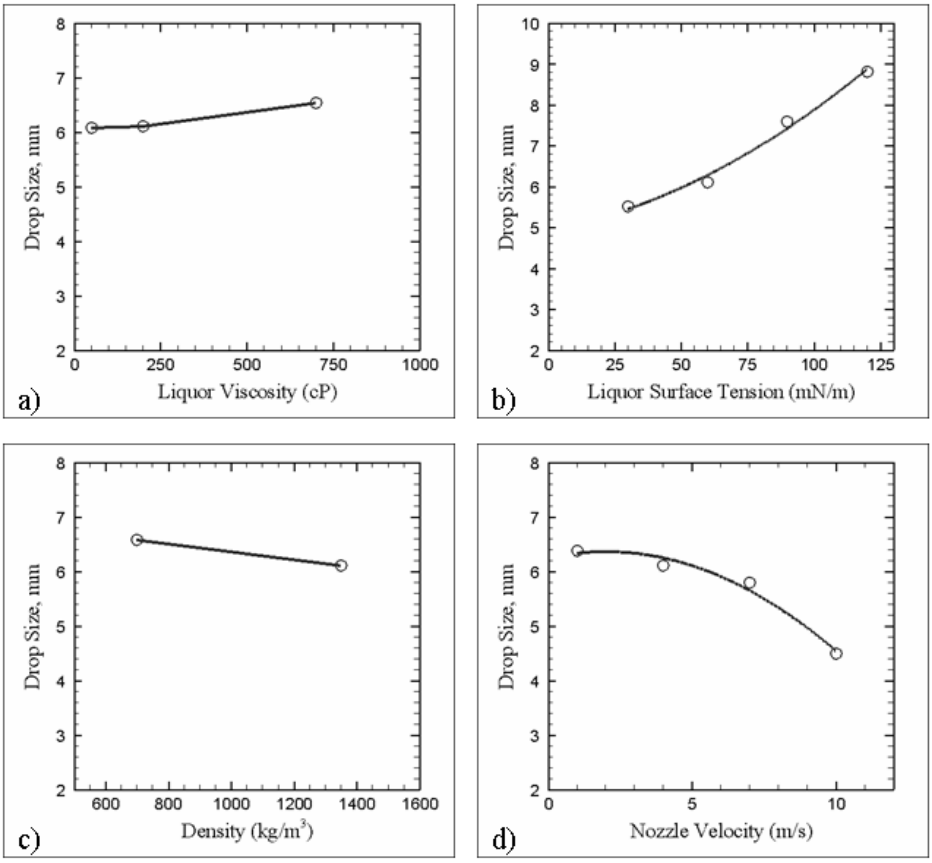

Fig. 15 The effects of black liquor properties and nozzle velocity on spray mean drop size (a) viscosity, (b) surface tension, (c) density, and (d) velocity. The unit cP for viscosity is *centi Poise*, which is equal to mPa·s.

velocity distributions along the angle from the plate centerline are obtained. The correlation then can be used to calculate the distribution of the spray mean drop size along this angle.

Nozzle Overall Characterization. In order to facilitate mesh generation and nozzle shape introduction, the *BLSpray* code is equipped with a preprocessor interface that links a commercial mesh generator called ICEM CFD to *BLSpray* input data. The three-dimensional CAD file of a black liquor splash-plate nozzle can be imported into ICEM CFD software for solid volume fraction definition and mesh generation. The ICEM–*BLSpray* interface generates

the output files that can be directly read by *BLSpray*. The computational mesh information and all boundary conditions, including the initial liquid inflow definition and nozzle velocity, are entered in this user-friendly interface.

BLSpray is also facilitated with an interface for postprocessing; the interface embedded in the code generates binary results that can be directly displayed using Tecplot software. This interface not only makes the postprocessing of the results more convenient, but also saves a large amount of disk space and reduces the processing time.

The results of the *BLSpray* computer program are in the form of digital files that include all the necessary information regarding the liquid location, velocity, and pressure in the whole computational domain. In order to get specific data from these results, such as the distribution of film thickness, film velocity, and spray flow, the *BLSpray* code has been equipped with a computer program module that automatically provides this information from *BLSpray* output files. The introduced correlation between film characteristics and spray drop size is also included in this program module in order to get spray drop size distribution. The developed program module for analyzing *BLSpray* results provides the following specific film and spray information:

- Mass median diameter (MMD) for the splash-plate nozzle
- Film thickness distribution at the nozzle exit against angle from the plate centerline
- Film velocity distribution at the nozzle exit against angle from the plate centerline
- Spray mean drop size distribution against angle from the plate centerline
- Spray flow distribution at each desired angle increment measured from the plate centerline

For the typical ALSTOM splash-plate nozzle considered in this paper, with conditions similar to those mentioned in the previous section (black liquor as fluid) but with a 5 m/s nozzle velocity, the results of the program module are shown in Fig. 16. The *BLSpray* code was first run for the nozzle on a small computational domain, and when the film thickness at the nozzle exit plane reached steady state, the simulation was terminated. The final output of *BLSpray* was saved in a certain file. A specific program module then extracted information from this file and, based on the developed correlations, provided the film and spray characteristics as shown in Fig. 16. The mass median diameter (MMD) obtained for this case was 5.44 mm. Therefore, half of the volume of spray contained droplets larger than the MMD, and the other half contained smaller droplets.

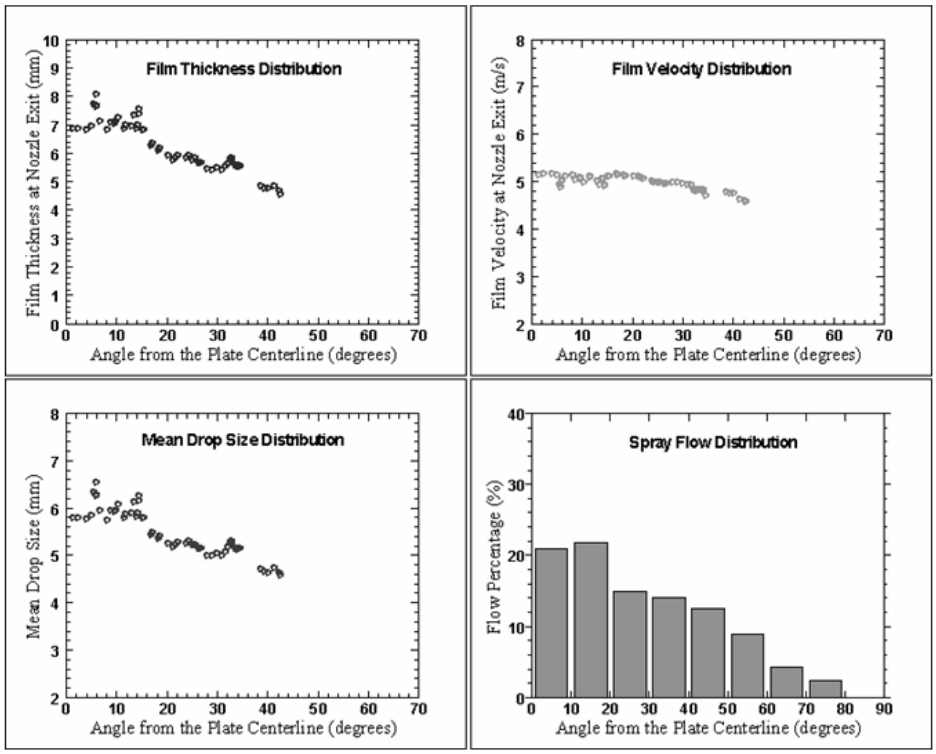

Fig. 16 The distribution of film thickness, film velocity, spray mean drop size, and spray flow for a typical ALSTOM splash-plate nozzle. This data is obtained using a program module that analyzes the results of the *BLSpray* code.

At the time this paper was written, the numerical techniques in *BLSpray* did not consider secondary breakup. Therefore, the film and spray characterization presented in this paper is based on film primary breakup. In addition, the computer model did not include vaporization of the liquid that is evident when fired into a splash-plate atomizer of an operational recovery boiler. To predict the droplet size more accurately, it is necessary to include in the model factors that influence the spray in situ. Examples of such factors include the effects of heat transfer, vaporization, and secondary breakup. Work is continuing to improve the model to include these influences. This will improve the ability of the *BLSpray* code to predict droplet size more accurately for any operating condition.

CONCLUSIONS

A three-dimensional computational fluid dynamics method was developed for spray characterization of splash-plate atomizers using numerical simulations. The method can be used to improve the design of current splash-plate nozzles, test new nozzle designs, and determine the effects of varying fluid properties and operating conditions on spray characteristics of a nozzle. The developed code, called *BLSpray*, was validated against laboratory experiments. This paper presents the numerical techniques used in the code and the results of the model validation.

The code was used to simulate the spray drop size distribution for a typical ALSTOM splash-plate nozzle. The effects of some of the main parameters, such as nozzle diameter, nozzle angle, and nozzle velocity, on the spray pattern were investigated.

Correlations were developed between liquid film characteristics at the nozzle exit and the spray mean drop sizes. The results of the *BLSpray* code were combined with these correlations to get film and spray characteristics while using less computational time and effort. This capability, along with the program module developed for analyzing the output data, have turned *BLSpray* into an efficient and practical tool for numerical characterization of splash-plate nozzles. This tool is used to understand the effects of black liquor properties and nozzle shape on droplet size and flow distribution.

The computer model did not include droplet secondary breakup in the airflow. Heat transfer and vaporization of liquid were also not considered. These factors are important in black liquor atomization in a chemical recovery boiler. Therefore, to accurately predict actual droplet size, it is necessary to include in the model factors that influence the black liquor spray in situ. Examples of such factors include the effects of heat from radiation and flue gases, as well as vertical gas velocity in the boiler. Work is continuing to improve the model to include these influences.

REFERENCES

1. W. W. Hagerty and J. F. Shea, A Study of the Stability of Plane Fluid Sheets, *J. Appl. Mech.*, vol. 22, pp. 509–514, 1955.
2. B. E. Dixon, A. W. Russell, and J. E. Swallow, Liquid Films Formed by Means of Rotating Disks, *Br. J. Appl. Phys.*, vol. 3, pp. 115–119, 1952.

3. N. Dombrowski, D. Hasson, and D. E. Ward, Some Aspects of Liquid Flow through Fan Spray Nozzles, *Chem. Eng. Sci.*, vol, 12, pp. 35–50, 1960.
4. R. P. Fraser, P. Shea, N. Dombrowski, and D. Hasson, Drop Formation from Rapidly Moving Liquid Sheets, *AIChE J.*, pp. 672–680, 1962.
5. N. Dombrowski, and W. R. Johns, The Aerodynamic Instability and Disintegration of Viscous Liquid Sheets, *Chem. Eng. Sci.*, vol. 18, pp. 203–214, 1963.
6. G. D. Crapper, N. Dombrowski, and G. A. D. Pyott, Large Amplitude Kelvin–Helmholtz Waves on Thin Liquid Sheets, *Proc. R. Soc. Lond., Ser. A*, vol. 342, pp. 209–224, 1975.
7. J. C. P. Huang, The Break-up of Axisymmetric Liquid Sheets, *J. Fluid Mech.*, 43, pp. 305–319, 1970.
8. C. D. Donaldson and R. S. Snedecker, A Study of Free Jet Impingement. Part 1. Mean Properties of Free and Impinging Jets, *J. Fluid Mech.*, vol. 45, pp. 281–319, 1971.
9. A. Mansour and N. Chigier, Disintegration of Liquid Sheets, *Phys. Fluids*, vol. 2, pp. 706–719, 1990.
10. A. Mansour and N. Chigier, Dynamic Behavior of Liquid Sheets, *Phys. Fluids*, vol. 3, pp. 2971–2980, 1991.
11. R. H. Rangel and W. A. Sirignano, The Linear and Nonlinear Shear Instability of a Fluid Sheet, *Phys. Fluids*, vol. 3, pp. 392–400, 1991.
12. I. Kim and W. A. Sirignano, Three-Dimensional Wave Distortion and Disintegration of Thin Planar Liquid Sheets, *J. Fluid Mech.*, vol. 410, pp, 147–183, 2000.
13. T. N. Adams, *Kraft Recovery Boilers*, chap. 4, TAPPI Press, Atlanta, 1997.
14. C. P. J. Bennington and R. J. Kerekes, The Effect of Temperature on Drop Size of Black Liquor Sprays, *J. Pulp Paper Sci.*, vol. 12, pp. J181–J186, 1986.
15. T. M. Spielbauer and T. N. Adams, Flow and Pressure Drop Characteristics of Black Liquor Nozzles, *Tappi J.*, vol. 73, no. 9, pp. 169–174, 1990.
16. A. Kankkunen, T. Helpio, and P. Rantanen, Small Scale Measurements of Black Liquor Spraying with Splashplate Nozzles, *Proc. of Tappi Engineering Conf.*, Tappi Press, Atlanta, GA, pp. 207–214, 1994.

17. H. L. Empie, S. J. Lien, W. Yang, and T. N. Adams, Spraying Characteristics of Commercial Black Liquor Nozzles, *Tappi J*., vol. 78, no. 1, pp. 121–128, 1995.
18. D. W. Loebker and H. J. Empie, Independently Controlled Drop Size in Black Liquor Sprays using Effervescent Atomization. Part II: Splashplate Nozzles, *J. Pulp Paper Sci*., vol. 28, pp. 251–258, 2002.
19. P. Miikkulainen and A. Kankkunen, The Characteristics of Black Liquor Sprays, *Colloquium on Black Liquor Combustion and Gasification*, Park City, UT, May, 2003.
20. C. W. Hirt and B. D. Nichols, Volume of Fluid (VOF) Method for the Dynamics of Free Boundaries, *J. Comput. Phys*., vol. 39, pp. 201–225, 1981.
21. D. L. Youngs, An Interface Tracking Method for a 3D Eulerian Hydrodynamics Code, Technical Report No. 44/92/35, AWRE, 1984.
22. M. Bussman, J. Mostaghimi, and S. Chandra, On a Three-Dimensional Volume Tracking Model of Droplet Impact, *Phys. Fluids*, vol. 11, pp. 1406–1417, 1999.
23. M. Pasandideh-Fard, Ph.D. Thesis, Department of Mechanical and Industrial Engineering, University of Toronto, 1998.
24. M. Pasandideh-Fard, M. Bussman, S. Chandra, and J. Mostaghimi, Simulating Droplet Impact on a Substrate of Arbitrary Shape, *Atomization and Sprays*, vol. 11, pp. 397–414, 2001.
25. N. Ashgriz, R. Washburn, and T. Barbat, Segregation of Drop Size and Velocity in Jet Impinging Splash Plate Atomizers, *Int. J. Heat Fluid Flow*, vol. 17, pp. 509–516, 1996.
26. T. Azuma and T. Wakimoto, Stochastic Study of Perforation in a Liquid Film Induced by Laminar–Turbulent Transition, *4th Int. Conference on Multiphase Flow*, June, 2001.
27. N. Obuskovic and T. N. Adams, Fluid Sheet Thickness and Velocity at the Tip of a Black Liquor Splash Plate Nozzle, *AIChE Annual Meeting*, San Francisco, Nov., 1989.